Two-Photon Coherent Transients

Two-photon nutation, free-induction decay, and population inversion by adiabatic rapid passage have been studied in NH_3 . These effects are easily visualized with a vector model. Relaxation times T_1 and T_2 have been measured.

A. Introduction

The study of resonant coherent interactions between radiation and matter has been a fruitful area of research since the early days of nuclear magnetic resonance spectroscopy [1]. Many of these spin resonance effects have since been developed into powerful analytical tools for everyday use in many areas of science and technology.

With the invention of the laser there has been much interest in studying the optical analogues of these resonance effects. Many interesting effects have been observed [2]. Precise measurements of relaxation times in diverse physical systems have been made, especially since the introduction of the powerful Stark switching and laser frequency switching techniques by Brewer and his coworkers [3]. The vector model of Feynman, Vernon, and Hellwarth [4] has been a very powerful tool in the visualization and theoretical understanding of many coherent optical phenomena.

Following the pioneering theoretical work of Hartmann [5] there has been much interest in two-photon coherent effects. These are transitions between states inaccessible by one-photon interaction, e.g., those of the same parity. Among the many theoretical papers on coherent two-photon effects are those of Belenov and Poluektov [6], Takatsuji [7], Brewer and Hahn [8], and Grischkowsky, Loy, and Liao (GLL) [9]. There have also been many experimental observations of various two-photon coherent effects [10-20]. Parallel to the laser experiments, there has also been much experimental interest in multiquantum spin resonances [21, 22].

In this article, we restrict ourselves to our own twophoton experiments on a two-photon transition in NH_a. We describe our measurements of the two-photon phase relaxation time T_2 and the population relaxation time T_1 using these coherent transients. New results on the effect of buffer gas are presented. These two-photon transients are also shown to be in excellent agreement with the theoretical predictions of the two-photon vector model of GLL [9].

In Section B, we briefly review the two-photon vector model of GLL. The two-photon transient experiments are described in Section C, followed by a short discussion and conclusion in Section D.

B. Theory of the two-photon vector model

The theoretical development of the two-photon vector model has been described in detail by GLL. Here we follow the method described in Section IIB of GLL; the basis of this method has been discussed earlier by Heitler [23]. The mathematical formulation will not be repeated. Instead, we look at a much simplified three-level system, shown in Fig. 1. Following the prescribed transformation procedure in GLL, we obtain a two-photon vector model for this simple system. We discuss the assumptions used, as well as the physical significances of these assumptions. While this simplified system is much less general than that described in GLL, its predictions were in excellent agreement with our experimental results, as shown in Section C.

Consider the three-level system in Fig. 1. The transitions $|1\rangle \leftrightarrow |3\rangle$ and $|3\rangle \leftrightarrow |2\rangle$ are assumed to be dipole-allowed, while the transition $|1\rangle \leftrightarrow |2\rangle$ is dipole-forbidden. The sum of the two input light frequencies $\omega_1 + \omega_2$ is assumed to be near or on the two-photon resonance Ω_{12}

Copyright 1979 by International Business Machines Corporation. Copying is permitted without payment of royalty provided that (1) each reproduction is done without alteration and (2) the *Journal* reference and IBM copyright notice are included on the first page. The title and abstract may be used without further permission in computer-based and other information-service systems. Permission to *republish* other excerpts should be obtained from the Editor.

 $\Omega_1-\Omega_2$, with the two-photon frequency offset defined as $\delta\equiv\Omega_{12}-(\omega_1+\omega_2)$. We further make the convenient assumptions that ω_1 is much more near resonance with the transition $|1\rangle\leftrightarrow|3\rangle$ than with the transition $|3\rangle\leftrightarrow|2\rangle$, and vice versa with ω_2 . Then the one-photon frequency offset is defined as $\Delta\equiv\Omega_{32}-\omega_2$, and $\Delta\approx\omega_1-\Omega_{13}$ if $\delta<<\Delta$.

We are interested in the two-photon coherent transient effects between states $|1\rangle$ and $|2\rangle$ induced by the input light beams ω_1 and ω_2 . Intuitively, one expects that if the one-photon offset Δ were "sufficiently large" (to be defined more precisely later), state $|3\rangle$ would hardly be excited, and one might be able to reduce the problem again to a two-level system involving only states $|1\rangle$ and $|2\rangle$. This would be most desirable since in the classic paper of Feynman, Vernon, and Hellwarth [4] it is shown that any two-level system can be represented by a vector model with an equation of motion identical to the well-known case of a spin in a magnetic field. This two-level reduction, however, clearly cannot be carried out on the Hamiltonian $\mathcal H$ using the unperturbed wave functions of the material system as the basis set, since in this basis set

$$\mathcal{H} = \begin{bmatrix} \hbar\Omega_1 & 0 & \frac{-P_{13}\varepsilon_1 \exp{(-i\omega_1 t)}}{2} \\ 0 & \hbar\Omega_2 & \frac{-P_{23}\varepsilon_2 \exp{(i\omega_2 t)}}{2} \\ \\ \frac{-P_{31}\varepsilon_1 \exp{(i\omega_1 t)}}{2} & \frac{-P_{32}\varepsilon_2 \exp{(-i\omega_2 t)}}{2} & \hbar\Omega_3 \end{bmatrix}.$$

The element connecting states $|1\rangle$ and $|2\rangle$ is zero. It is therefore necessary to go into a new basis set where the states are mixtures of the original states, this mixture being induced by the input fields ε_1 and ε_2 . The new Hamiltonian is then obtained via unitary transformations described in detail in GLL. The result for our simplified three-level system is

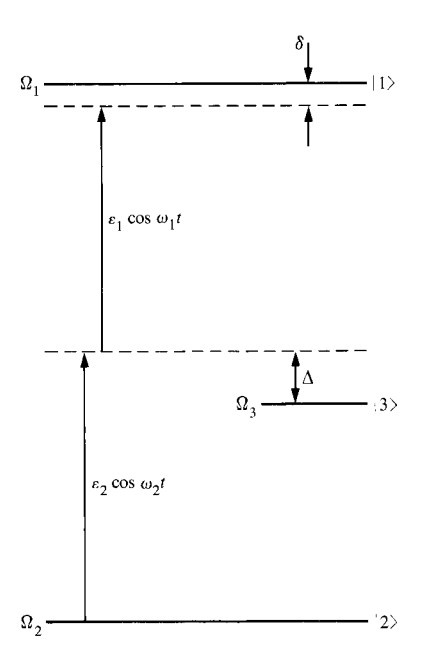


Figure 1 Schematic energy diagram of the simplified three-level system.

$$\Delta E_2 = \frac{|P_{23}\varepsilon_2|^2}{4\hbar^2\Delta} \,. \label{eq:delta_E2}$$

These are simply the well-known ac Stark shifts due to the input light fields ε_1 and ε_2 . These shifts are expected since physically the new basis states correspond to the original basis set interacting with the light fields. Third, it is evident that when the frequency factor $(\omega_1+\omega_2)$ in \mathcal{H}_{12}'' is close to the energy difference $\mathcal{H}_{11}''-\mathcal{H}_{22}''$, there is strong resonance enhancement, allowing us to neglect the contribution from \mathcal{H}_{13} even when $|\mathcal{H}_{13}''|$ is larger than $|\mathcal{H}_{12}''|$. This three-level problem is thus reduced to a two-level problem.

Before proceeding to the two-photon vector model, we discuss the restrictions needed to reduce the system to a

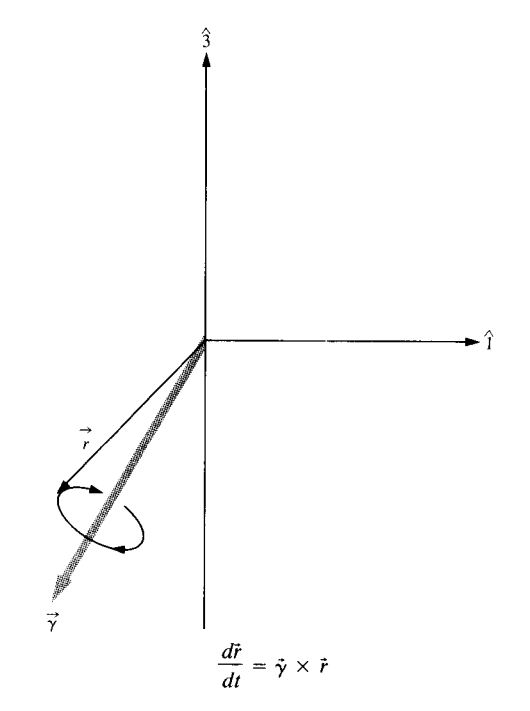
$$\mathcal{H}'' = \begin{bmatrix} \hbar\Omega_1 + \Delta E_1 & \frac{-P_{13}P_{32}\varepsilon_1\varepsilon_2}{4\hbar^2\Delta} \exp\left[-i(\omega_1 + \omega_2)t\right] & \frac{-P_{13}\varepsilon_1 \exp\left(-i\omega_1t\right)}{2} \\ \frac{-P_{13}P_{32}\varepsilon_1\varepsilon_2}{4\hbar^2\Delta} \exp\left[i(\omega_1 + \omega_2)t\right] & \hbar\Omega_2 + \Delta E_2 & \frac{-P_{23}\varepsilon_2 \exp\left(i\omega_2t\right)}{2} \\ \frac{-P_{31}\varepsilon_1 \exp\left(i\omega_1t\right)}{2} & \frac{-P_{32}\varepsilon_2 \exp\left(-i\omega_2t\right)}{2} & \hbar\Omega_3 - \Delta E_1 - \Delta E_2 \end{bmatrix}.$$

Several important features of this transformed Hamiltonian deserve attention. First, the element \mathcal{H}''_{12} is no longer zero. Second, the eigenenergies are shifted by

$$\Delta E_1 = -\frac{|P_{13}\varepsilon_1|^2}{4\hbar^2\Lambda},$$

two-level problem. The first two restrictions enter into the unitary transformation leading to \mathcal{H}'' . As discussed in

505



1-Photon

2-Photon

$$\begin{split} \gamma_1 &= -\kappa \varepsilon, \qquad \kappa = P_{12}/\hbar \qquad \gamma_1 = -\kappa \varepsilon_1 \varepsilon_2, \qquad \kappa = |P_{13} P_{32}/2 \hbar^2 \Delta| \\ \gamma_2 &= 0 \qquad \qquad \gamma_2 = 0 \\ \gamma_3 &= \Omega_{12} - \omega \qquad \qquad \gamma_3 = \Omega_{12} - (\omega_1 - \omega_2) \\ &+ (\Delta E_1 - \Delta E_2)/\hbar \end{split}$$

Figure 2 Pictorial representation of the vector model. The expression for $\vec{\gamma}$ in the one-photon case assumes input light $\varepsilon\cos\omega t$ near-resonant with a two-level system with transition moment P_{12} and energy separation Ω_{12} .

GLL, if the fields ε_1 and ε_2 are turned on adiabatically with respect to the intermediate state, i.e., $(1/\varepsilon_i)\partial\varepsilon_i/\partial t < \Delta$, i=1,2, the transformation operator can be expanded into a power series in S, where in our three-level system $|S|=P_{i3}\varepsilon_i/\hbar\Delta$, i=1,2. For this series to converge, |S| must be less than 1. The physical significances of these two restrictions,

$$\Delta > \left(\frac{1}{\varepsilon_i}\right) \frac{\partial \varepsilon_i}{\partial t}$$
 and (1a)

$$\Delta > \frac{P_{i3}\varepsilon_i}{\hbar} \qquad i = 1, 2, \tag{1b}$$

are quite clear. It defines our intuitive expectation that Δ should be "sufficiently large." Equation (1a) states that Δ should be sufficiently large that as the fields are turned on and off, the Fourier sidebands will not transiently excite

the intermediate state. As steady state is approached, Eq. (1b) states that the interaction strength between states $|i\rangle$ and $|3\rangle$ induced by ε_i , given by $P_{i3}\varepsilon_i/\hbar\Delta$, should be small. In fact, if the system is initially in the ground state $|2\rangle$, the population in $|3\rangle$ is given by $(P_{23}\varepsilon_2/\hbar\Delta)^2$, provided that this factor is small compared to 1. Therefore, physically speaking, these restrictions require that Δ be sufficiently large for one-photon interaction with the intermediate state to be small. The third restriction is self-evident:

$$\omega_1 + \omega_2 \approx \Omega_{12}$$
.

This provides the two-photon resonance enhancement so that the system can be reduced to a two-level problem.

We now apply the vector model of Feynman, Vernon, and Hellwarth to this two-level problem. In this model, the response of the material system to the light is described by the precession of a unit vector \vec{r} about the $\vec{\gamma}$ vector,

$$\frac{d\vec{r}}{dt} = \vec{\gamma} \times \vec{r}. \tag{2}$$

The formalism therefore becomes equivalent to that of spin resonance and one-photon coherent optics. In the "rotating coordinate frame" the components of $\vec{\gamma}$ for our system are

$$\gamma_1 = -\kappa \varepsilon_1 \varepsilon_2,\tag{3a}$$

$$\gamma_{2} = 0, \tag{3b}$$

$$\gamma_3 = \Omega_{12} - (\omega_1 + \omega_2) + (\Delta E_1 - \Delta E_2)/\hbar,$$
 (3c)

where

$$\kappa = |P_{13}P_{32}/2\hbar^2\Delta| \tag{3d}$$

and

$$\Delta E_i = -|P_{i3}\varepsilon_i|^2/4\hbar\Delta \qquad i = 1, 2. \tag{3e}$$

The components of \vec{r} have the usual physical meaning analogous to those of the one-photon vector model and spin resonances; r_1 is the in-phase polarization, r_2 is the out-of-phase polarization, and r_3 is the population difference between states $|1\rangle$ and $|2\rangle$.

As depicted in Fig. 2, except for different expressions for $\vec{\gamma}$, the one-photon and two-photon vector models have the *same* equation of motion. This formal similarity has important consequences. In the absence of propagation effects, many one-photon coherent processes, such as optical free precession, echoes, adiabatic following and adiabatic inversion, can be described by the vector model alone. These clearly have their two-photon analogues. In fact, the conditions for these processes, expressed in terms of $\vec{\gamma}$ and \vec{r} , are identical for the one- and two-photon processes. For coherent propagation effects such as

self-induced transparency, the vector model must be coupled with the Maxwell equations. For the two-photon case, two optical fields are coupled with the vector model. Due to the presence of this additional field, and also the optical Stark shift terms in γ_3 , it is difficult to ascertain, without detailed analysis, whether a given one-photon coherent propagation effect will have its two-photon analogue. In this paper we confine ourselves to non-propagating two-photon coherent transients.

We now discuss several features of the vector model that are particular to the two-photon process and compare these to the one-photon process. First, γ_2 in the twophoton case contains the extra terms corresponding to the optical Stark shifts. Thus, the instantaneous two-photon frequency offset γ_3 becomes intensity-dependent. Further, if pulsed lasers are used in the experiment, γ_3 becomes time-dependent. Second, in the two-photon case, it is possible to greatly reduce the inhomogeneous linewidth due to Doppler broadening by using two counterpropagating beams. This greatly enhances the two-photon transient signal since, unlike the one-photon case where the laser light only interacts with the small portion of the molecules that travel at a particular velocity, here all molecules interact with the input light waves, independent of their velocities. In addition, dephasing relaxation times that are longer than T_2^* because of Doppler broadening can now be observed directly. This is a very important advantage over the one-photon process. The third feature concerns the experimental observation of twophoton transients. Unlike one-photon polarization, twophoton polarization does not radiate by itself. However, it can be detected in the presence of an input field at ω_i , resulting in a radiation at the complementary frequency $(\Omega_{12} - \omega_i)$. Finally, the two-photon interaction strength is smaller than the one-photon interaction strength. From the one- and two-photon expressions for γ_1 (see Fig. 2), one sees that the two-photon interaction strength is roughly reduced by a factor of $P_{i3}\varepsilon_i/\hbar\Delta$, which is just our expansion parameter and must be small compared to unity. Experimentally, however, if this factor is ≈ 0.1 , the reduction in interaction strength is more than compensated by the increase in signal for the Doppler width reduction, as seen in Section C.

Before proceeding to the experimental section, we briefly discuss the possible extensions of the two-photon vector model. While the procedure in GLL is valid for the two-photon process, the more general method of eliminating the intermediate states described by Heitler [23] is valid for multiphoton processes. It should be straightforward to apply Heitler's method, along the direction in GLL, to yield a multiphoton vector model. Recently, Friedmann and Wilson-Gordon [24] have also extended

the two-photon vector model to a multiphoton vector model by using projection operator techniques. Finally, a generalized two-photon theory has been given by Schenzle and Brewer [25] from which nonperturbative solutions can be obtained.

C. Two-photon coherent transient experiments in NH₂

As discussed in Section B, the two-photon vector model predicts that for every nonpropagating one-photon transient effect there should be a two-photon analogue. To check these predictions experimentally, one needs a physical system with known spectroscopy and transition moments. It should have a two-photon transition that is near or on resonance with the sum of two laser frequencies. Further, the location of the intermediate state should be such that the one-photon offset Δ should be "sufficiently large," as defined above. Yet Δ should not be too large, for otherwise the two-photon interaction strength will be too small.

The system we have chosen satisfies all of the above requirements. The NH₂ transition $(\nu_2, J, K) = (0^-, 5, 4) \rightarrow$ $(2^-, 5, 4)$ is one-photon-forbidden since $\Delta \nu = 2$ and both states have the same parity. This transition is near-resonant with the sum of the CO, laser lines P34 and P18 at frequencies of 27 910 721 MHz and 28 359 774 MHz, respectively. The two-photon frequency offset has been accurately measured to be 294.37 MHz, and the one-photon frequency offset Δ between the P34 line and the intermediate state (1⁺, 5, 4) has been determined to be 5250 MHz. The frequencies of the laser lines are sufficiently different that the ground-to-intermediate state transition is only near-resonant with the P34 line and the intermediate-to-upper state transition is only near-resonant with the P18 line. While this difference in frequencies produces a residual Doppler width even with the counterpropagation geometry, this residual width is only ≈2 MHz (compared to the original Doppler width of 160 MHz).

In the absence of fields, all three states have M degeneracies of 2J+1. The transition moment of each M sublevel is proportional to |M| and thus varies substantially among the sublevels. For quantitative comparisons with theory, it is most desirable to remove this degeneracy. Also, at zero field, the two-photon frequency offset of 294 MHz is many times larger than the 2-MHz linewidth of the system and any two-photon excitation will be extremely small. Application of an external field solves both of these problems. Due to the M dependence of the Stark effect, the $M=\pm 5$ sublevels can be selectively shifted on resonance. Effects from all other M states can be neglected since they are many times the two-photon line-

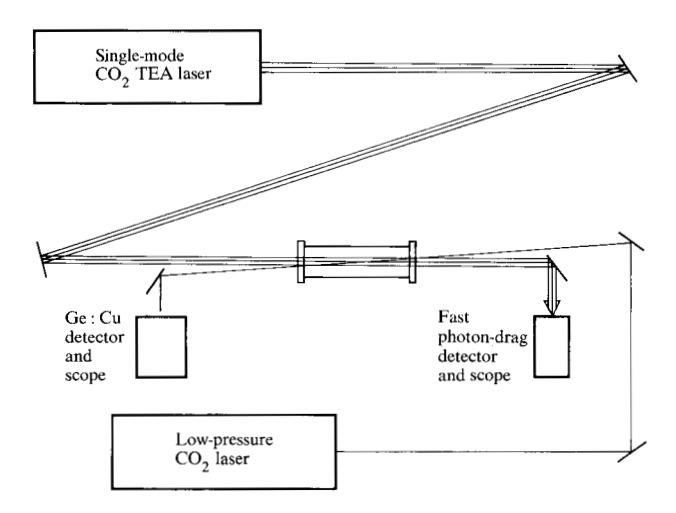


Figure 3 Schematic diagram of the experimental setup.

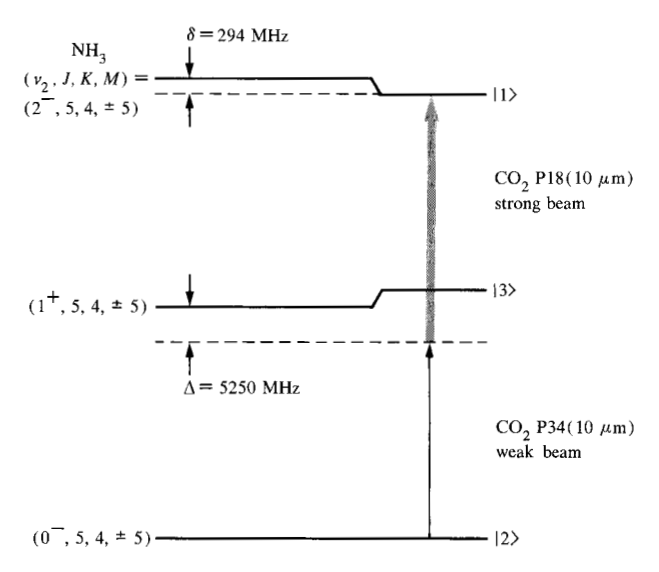


Figure 4 Energy level diagram of the NH₃ two-photon transition and the near-resonant CO₂ laser frequencies.

width away. Thus, in the notation of Fig. 1, the states $|1\rangle$, $|2\rangle$, and $|3\rangle$ of our simplified three-level system are $(\nu_2, J, K, M) = (2^-, 5, 4, \pm 5), (0^-, 5, 4, \pm 5),$ and $(1^+, 5, 4, \pm 5),$ respectively. The dipole moments involved are then uniquely defined and known; $P_{13} = 0.17$ debye $(1 \text{ debye} = 10^{-18} \text{ statcoulomb-cm} = 3.336 \times 10^{-28} \text{ coulomb-cm})$ and $P_{23} = 0.16$ debye. As discussed in more detail later, this external field, which tunes the system on resonance and at the same time removes the M degeneracies, can be an applied electric field or even the laser input fields ε_1 and ε_2 themselves.

The experimental setup is shown in Fig. 3. Two CO_2 lasers were used. One of them was a grating-tuned CO_2

transverse-excitation atmospheric (TEA) laser. This commercially available laser (Tachisto 215G) had multilongitudinal mode output with a linewidth exceeding 1 GHz. It was absolutely essential to make the output single-mode for this type of experiment. This was achieved by the addition of a low-pressure section inside the cavity. This low-pressure section provided stimulated emission in a single longitudinal mode which then forced the TEA laser to preferentially go into this same longitudinal mode. The output of this hybrid TEA laser had a peak power of >1 MW and a pulse duration of about 100 ns. It was monitored by a fast photon-drag detector with a Tektronix 7904 oscilloscope. The other laser was a longitudinally pulsed low-pressure (≈ 10 torr or 10^3 Pa) CO_a laser also operating in a single longitudinal mode. (This pulsed laser, as well as the low-pressure section in the TEA laser, was of our own design and has been described in detail [26].) The output of this low-pressure laser had a duration of 150 μ s and could be considered cw in the time scale of this experiment (≈100 ns). The peak power was ≈100 W. The two counterpropagating beams interacted in an NH, gas cell whose pressure was monitored by a capacitive manometer (MKS Baratron). The weaker beam, after propagating through the cell, was detected by a fast photoconductor (Ge:Cu at 4.2 K) and another 7904 scope. Due to the very different power levels of the two lasers, it was necessary to pass the weak beam through an 0.5-m infrared spectrometer as a filter against stray reflections from the strong beam. Also, by means of a high-pass electrical filter, the 150-us-long weak-beam signal was suppressed in favor of the two-photon transient signal in the time scale of ≈ 100 ns.

We should point out that the choice of a pulsed strong beam ε_1 and a cw weak beam ε_2 has a number of advantages. First, the time-dependent optical Stark shift is entirely determined by the strong beam. Second, as discussed in Section B, observation of the two-photon polarization relies on its beating with, say, ω_1 , resulting in radiation of the complementary frequency ω_{o} . The magnitude of the transient signal on the weak beam is therefore proportional to the field strength of the strong beam. This results in a very good signal-to-background ratio. Finally, if the weak beam is nearly resonant with the transition between the ground and intermediate states and the strong beam nearly resonant with the transition between the intermediate and the final states, there can be little excitation in the intermediate state and parasitic onephoton resonant effects are effectively eliminated.

• Observation of two-photon free-precession decay via optical Stark shifting (Ref. [12])

It is clear from the expression for γ_3 in the vector model Eq. (3c) that the optical Stark shift plays an important

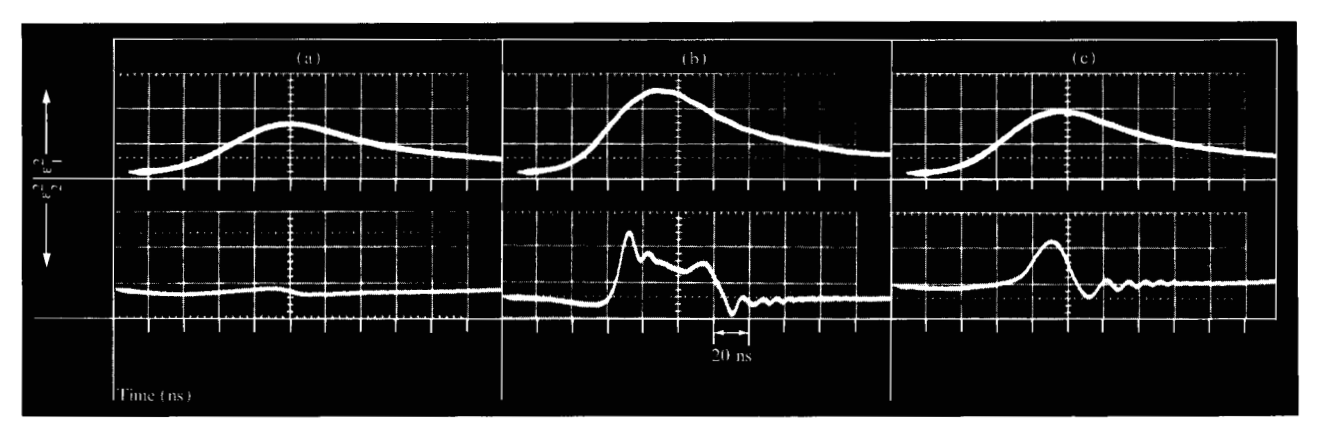


Figure 5 Two-photon coherent signals on the weak beam ε_2^2 at various strong-beam intensities ε_1^2 : (a) <1 MW/cm²; (b) >>1 MW/cm²; (c) intermediate case.

role in the two-photon problem. It determines the instantaneous two-photon offset; thus, its effect on any two-photon experiment must be anticipated and reckoned with. In this experiment, following an idea discussed by Grischkowsky and Loy [27], we take advantage of this effect to shift the two-photon transition on resonance. This is achieved by judiciously choosing ε_1 to be the strong beam and ε_2 to be the weak beam, as depicted in Fig. 4.

The phenomenon of free-precession decay is easily visualized by using the two-photon vector model. When the system is excited suddenly (or nonadiabatically) the polarization vector \vec{r} precesses about $\vec{\gamma}$ with the characteristic precession frequency $(\gamma_1^2 + \gamma_3^2)^{1/2}$. Generally, the term nutation signifies the precession process when $|\gamma_1| >> |\gamma_3|$ (i.e., on resonance), while the term free-induction decay is used when $|\gamma_3| >> |\gamma_1|$ (off resonance). In the present experiment the two-photon transition is shifted by the optical Stark effect on resonance and then off resonance, and the nutation effect evolves smoothly into free-induction decay. The more general term, precession, will be used to describe the entire process. This free precession gives rise to a time-varying out-of-phase polarization r_{s} . When beat with ε_{s} , this produces alternating absorption and emission of light on the weak beam ε_2 , which can be detected easily.

Using the known parameters of this NH₃ transition, it is easy to calculate the intensity needed in the strong beam to shift the two-photon transition on resonance with the sum of the input frequencies. With $\delta=294$ MHz, $P_{13}=0.17$ debye, and $\Delta=5250$ MHz, we found, by using Eq. (3e), that the optical Stark shift (the very small shift from the weak beam ε_2 being negligible) is equal to δ when $\varepsilon_1=0.15$

94.7 esu, corresponding to an intensity of about 1 MW/cm² for our linearly polarized beam.

In our experiment, data were obtained on a single-shot basis due to the slow repetition rate of <1 Hz imposed by the CO, TEA laser. Both lasers and the two Tektronix 7904 scopes were externally triggered, with various delays, by a master clock. Great care was taken to synchronize the two scope traces to within a few nanoseconds. Figure 5 shows a series of data at different strongbeam intensities. The NH₃ pressure in the 10-cm-long cell was 180 mtorr (24 Pa). Note that the photon-drag detector monitoring the strong beam gives a positive signal, while the Ge:Cu detector for the weak beam gives a negative signal. In Fig. 5(a) the peak intensity of the strong beam was below 1 MW/cm² and there was little two-photon interaction. Figure 5(b) shows the case where the strong-beam peak intensity substantially exceeded 1 MW/cm². Here, on the weak beam, we see two trains of oscillating two-photon precession signals. This is due to the fact that the molecules were brought through twophoton resonance once on the leading edge and again on the trailing edge of the pulse. However, between these two cases, if the strong-beam peak intensity corresponded exactly to that required to optically Stark shift the two-photon transition on resonance, only one train of precession signals appeared, as shown in Fig. 5(c). This is obviously the most desirable case for detailed theoretical analysis and comparison.

In general, this two-photon signal was found to be most sensitive to laser frequency purity. A small admixture of neighboring longitudinal modes to the strong beam produced severe effects on the two-photon signal. The signal was also found to be very sensitive to spatial overlap of

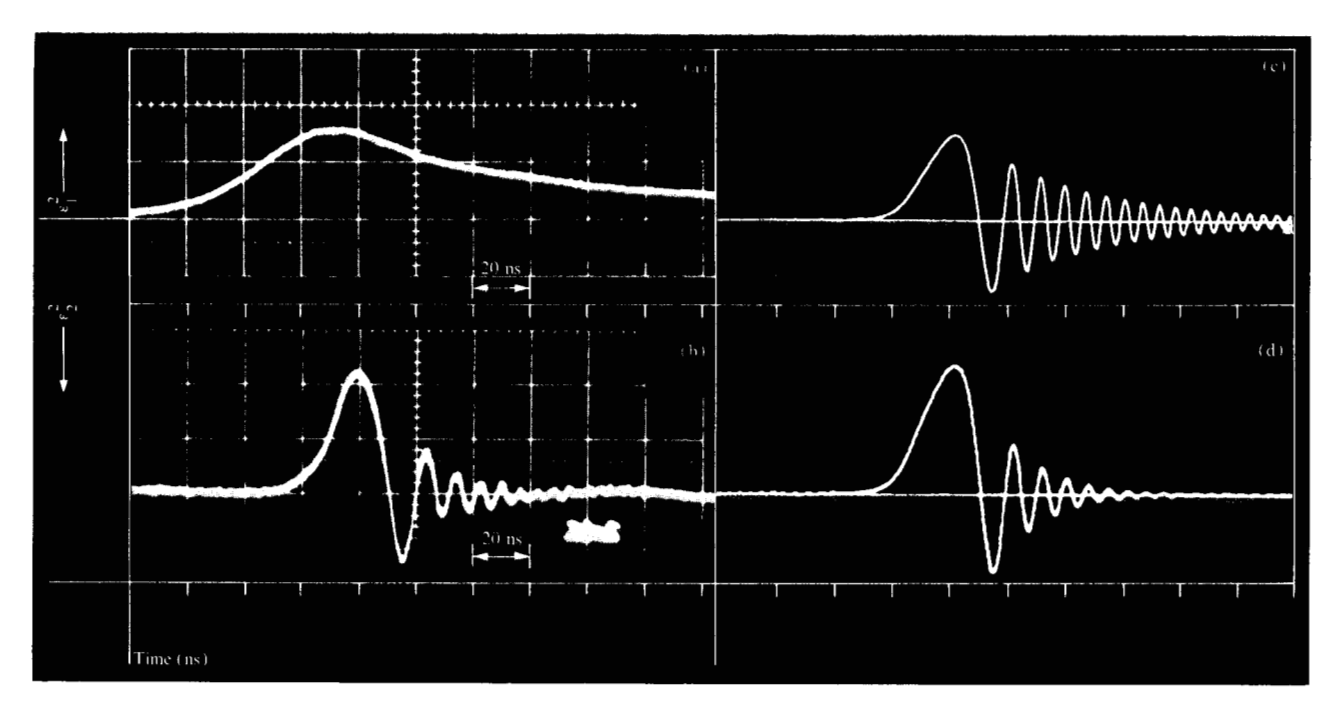


Figure 6 Two-photon coherent free-precession signal for (a) the strong beam ε_1^2 and (b) the weak beam ε_2^2 . (c) Theoretical calculation for the above case assuming spatially homogeneous $\varepsilon_1 = 94.7$ esu. (d) Theoretical calculation for the above case assuming a small spatial variation in the strong beam equal to ± 1 esu.

the two counterpropagating beams. Special precaution was also taken to ensure that spatial intensity variation of the strong beam was minimized over the entire cross section of the weak beam. This was done by having the strong beam passed through a 6-mm aperture and placing the 10-cm-long NH $_3$ cell in the far-field region of the aperture. The weak-beam diameter was reduced to 2 mm and intersected the central flat region of the strong beam. Note that the time behavior of the signal on the weak beam is independent of the intensity of the transverse spatial structure of the weak beam; however, the magnitude of the signal is linearly proportional to the weak-beam field strength ε_9 .

Figure 6 shows one of our best results on which theoretical comparisons were made. The peak power of the strong beam [Fig. 6(a)] was extremely close to, if not exactly equal to, that required to shift the two-photon transition on resonance. (A mere 5% reduction of the laser power caused the precession signal to decrease by a factor of three.) Note the interesting feature that the precession frequency increased with time, with the precession period decreasing from ≈ 20 to ≈ 5 ns. This is easily understood in terms of the vector model. The precession frequency $|\vec{\gamma}| = (\gamma_1^2 + \gamma_3^2)^{1/2}$ is a function of the optical Stark shift through γ_3 . Since the precession signal

was observed at the trailing edge of the TEA laser pulse, the precession frequency increased with time as the system shifted away from resonance. This was a result of the decreasing optical Stark shift accompanying the decreasing laser intensity. Note also that the observation of the precession periods would have been impossible without the Doppler width reduction, since these periods were much longer than the normal T_2^* of a few nanoseconds.

We now compare the experimental result to the theoretical prediction of the two-photon vector model, which is governed by the equation of motion [Eq. (2)]. With the system originally in the ground state, we have the initial condition $r_1(0) = 0$, $r_2(0) = 0$, and $r_3(0) = -1$. The components of $\vec{\gamma}(t)$ are

$$\gamma_1 = -\kappa \varepsilon_1(t) \varepsilon_2$$

$$\gamma_2 = 0$$
,

$$\gamma_3 = \delta - |P_{13}\varepsilon_1(t)|^2/4\hbar\Delta,$$

where $\kappa \equiv |P_{13}P_{32}/2\hbar\Delta|$. All material parameters are known. For this problem ε_2 can be considered to be independent of time, and it is easily shown that the exact magnitude of ε_2 , as long as it is small, is not material. On the other hand, both the exact magnitude and the time-dependence of $\varepsilon_1(t)$ are crucial inputs to the calculation. The

510

input time-dependence of $\varepsilon_1(t)$ was obtained by digitizing the waveform $\varepsilon_1^2(t)$ shown in Fig. 6(a). The exact magnitude of $\varepsilon_1(t)$, however, would be difficult to measure to better than 10% due among other factors to the exact calibration of the photon-drag detector and the spatial intensity distribution of the TEA laser beam. Fortunately, from the critical dependence of the precession signal strength on the peak power, the maximum value of ε , for the case in Fig. 6 can simply be set to be 94.7 esu so that molecules are on resonance at the pulse peak. The calculation now has no free parameters. The time-dependent \vec{r} can be obtained by numerically integrating the equations of motion (1) with the given initial conditions $\vec{r}(0)$. In the absence of propagation effects, the time-dependent twophoton precession signal observed on ε_0 is given by [see Eq. (54) of GLL]

$$\Delta \varepsilon_2(t) = \frac{2\pi\omega}{c} N\hbar\kappa r_2(t)\varepsilon_1(t)\ell,$$

where N is the number density of NH_3 and ℓ is the interaction length.

The result of this numerical calculation, assuming a phenomenological T_a relaxation of 35 ns, is shown in Fig. 6(c). The general features of this numerical result, especially the increasing precession frequency, agree well with the experimental result in Fig. 6(b). However, it is also immediately clear that the observed two-photon freeprecession signal decayed much faster than the collisioninduced T₂ of 35 ns deduced from two-photon line-broadening data. This fast decay was due to the finite spatial variation of ε_1 over the 10-cm-long interaction region. While every effort was made to keep ε , constant, it would be unrealistic to assume a variation in $\varepsilon_{1}(z)$ to be less than $\pm 1\%$, especially since ε_1 and ε_2 are not exactly counterpropagating. Through the optical Stark effect, this ±1% variation in ε , produces an inhomogeneous broadening of about ±6 MHz. Figure 6(d) shows the result of a numerical calculation assuming the collisional relaxation time $T_2 = 35$ ns and the spatial variation of $\varepsilon_1(z)$ to be $\pm 1\%$ over the interaction region. The result is now in excellent agreement with the observed waveform.

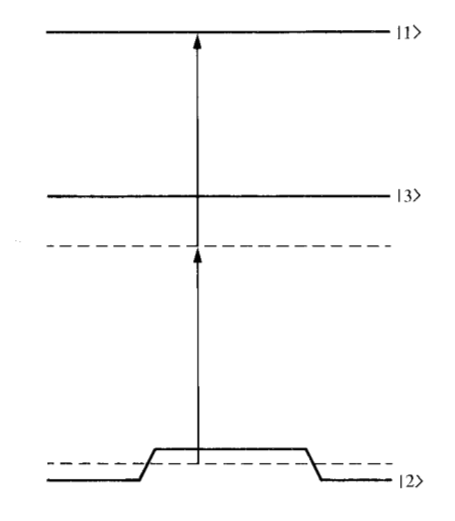
This is the first experimental observation of the two-photon analogue of the familiar one-photon free-precession decay process. It demonstrates the crucial roles of the two processes unique to the two-photon problem: the optical Stark effect and the Doppler width reduction by counterpropagating beams. The excellent agreement with the prediction of the two-photon vector model provides the first quantitative confirmation of this model and clearly points to the possible observations of other two-photon coherent effects such as adiabatic inversion and echoes.

• Two-photon free-precession decay by Stark switching and measurements of the two-photon phase relaxation time T_{\circ} (Ref. [15])

The study of transient coherent effects has, since the early work in nuclear magnetic resonance, been most fruitful in yielding precise and detailed information on the relaxation times of physical systems. Our study of twophoton coherent transients, while primarily due to the interesting and novel physical phenomena involved, was also motivated by the potential use of such transients for measuring relaxation times of two-photon transitions that are not accessible by one-photon excitation. The experiment described in the last section, with the two-photon transition shifted on resonance by the input light fields via the optical Stark effect, allows us to observe the physical phenomena and to compare them quantitatively with theory without the use of free parameters. Despite its simplicity and beauty, it is clear that this technique would be most difficult for measurement of relaxation times. First, as shown previously, the two-photon precession signal depends critically on both the amplitude and the shape of the TEA laser pulse. In our experiment, the shot-to-shot variations of the amplitude and the pulse shape were at least $\pm 10\%$. As a result the two-photon precession signal varied greatly. Without significantly improving the TEA laser output reproducibility, one would have to correct for this variation before accurate relaxation times could be obtained. Second, through the optical Stark effect, any spatial variations in the TEA laser beam can produce significant inhomogeneous broadening. This is particularly detrimental for relaxation time measurements, since this inhomogeneous broadening changes from shot to shot because of laser output transverse-mode fluctuations. It would be extremely difficult to monitor or to correct for such fluctuations.

The cause of these two difficulties can be traced to the use of the optical Stark effect to shift the transition on resonance. To avoid this, in the present experiment we use the Stark switching technique of Brewer and coworkers [3], which has been demonstrated to be of great importance in the study of one-photon transients. Our experiment is in fact closely related to that first suggested in the theoretical paper of Brewer and Hahn [8].

The same two-photon transition in NH_3 , together with the same CO_2 laser lines, was used in this experiment. The weak-beam characteristics at the P34 line remained unchanged as before. The strong-beam characteristic, however, was changed. Previously, the laser gave a 100-ns, 1-MW power pulse. By suitably adjusting the relative timing between the low-pressure and the TEA discharge sections, we obtained an output pulse of ≈ 1 - μ s duration and 100-kW peak power. This reduced strong-beam in-



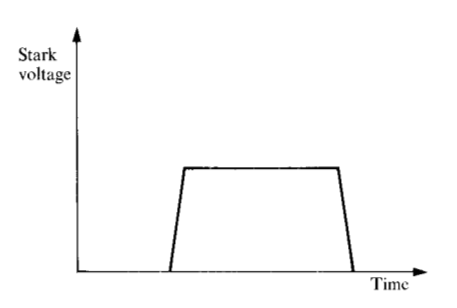


Figure 7 Schematic energy diagram for two-photon Stark switching experiment.

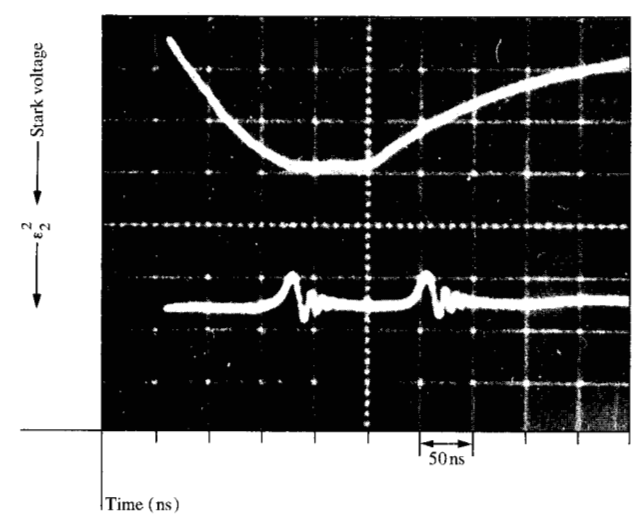


Figure 8 Stark switched two-photon free precession (lower trace) together with the Stark pulse (upper trace).

tensity, while also reducing the magnitude of the precession signal, produced a maximum optical Stark shift of only ≈ 30 MHz. More importantly, the inhomogeneous

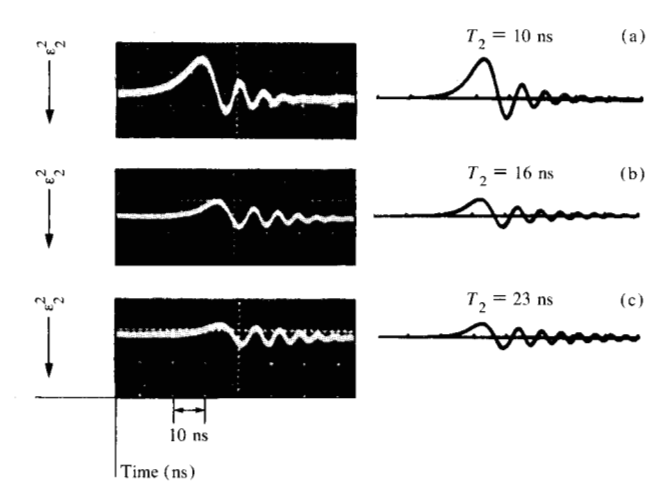


Figure 9 Stark switched two-photon free precession at decreasing NH₃ gas pressures (a) 866 mtorr (115 Pa), (b) 565 mtorr (75 Pa), and (c) 336 mtorr (45 Pa).

broadening due to spatial variation of the strong-beam intensity was in this case reduced to less than 1 MHz (which is negligible in this experiment). Also, at the much longer pulse width of 1 μ s, both lasers could effectively be considered cw in the time scale of the experiment. The timing of the experiment was then entirely controlled by the external Stark pulses. Due to the inversion doublets in the $v_2 = 0$ ground vibrational band in NH₃, the states in this band have relatively large dc Stark coefficients. The electric field needed to shift this two-photon transition on resonance with the sum of the CO₂ laser lines has been measured to be 5253 V/cm. The energy levels are shown schematically in Fig. 7. The 10-cm-long Stark plates were separated by precision 2-mm spacers. The two lasers, counterpropagating to each other, were both linearly polarized along the direction of the external Stark field. As before, the two-photon precession signal was monitored by detecting the weak beam after it had passed through the Stark cell.

Figure 8 shows a typical Stark switched two-photon precessing signal (lower trace) together with the Stark voltage (upper trace). The precession signals induced at the rising and trailing edges of the Stark pulse were independent for this relatively long Stark pulse duration. The signal was stable and repeatable from shot to shot. Varying the rise and fall times of the Stark pulse resulted in the expected changes of the precession frequencies. The precession decay time was a function only of the gas pressure. While changes in laser intensities affected the magnitudes of the signals, neither the precession frequency nor the decay time was affected. Thus, unlike the experiment in the previous subsection, measurement of the two-photon relaxation time is now possible.

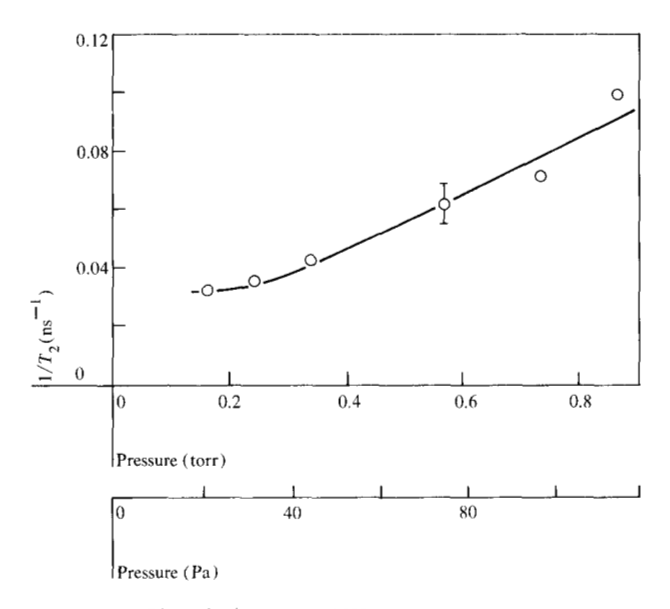


Figure 10 Plot of $1/T_2$ versus NH_3 pressure.

Figure 9 shows typical two-photon precession signals at decreasing pressures of NH_3 . For clarity, only the precession signals at the trailing edge of the Stark pulse are shown. The Stark pulse used in all three cases had an amplitude of 1200 V with an exponential fall time of 47.5 ns. By using the two-photon vector model and the known physical parameters, the precession signals were calculated for different values of the relaxation time. The theoretical fits for the experimental traces are shown next to each trace. The values of T_2 used in the calculations were (a) 10, (b) 16, and (c) 23 ns.

The inverse values of the relaxation times thus obtained were plotted versus pressure in Fig. 10. This figure shows that above 0.2 torr (\approx 27 Pa) $1/T_2$ increases linearly with pressure, yielding a collision-induced relaxation time of $T_2p = 10.5 \pm 2$ ns-torr (1400 ± 270 ns-Pa), where p is the pressure of NH₃ in torr (Pa). Below 0.2 torr the decay time was apparently limited by dephasing mechanisms other than collision. The limiting value of 0.03 (ns)^{-1} for $1/T_a$ corresponded to a linewidth of about 10 MHz and was higher than that expected from the residual Doppler width or the laser linewidth. This almost certainly was due to the nonuniform strong-beam intensity inside the Stark cell, being zero at the Stark plates and maximized at the midpoint between them. With the strong-beam intensity at about 100 kW/cm², this could produce an inhomogeneous broadening as large as 30 MHz. This inhomogeneous broadening, however, was not a serious problem because it did not fluctuate from shot to shot. This was the first time-domain relaxation time measurement for a two-photon transition.

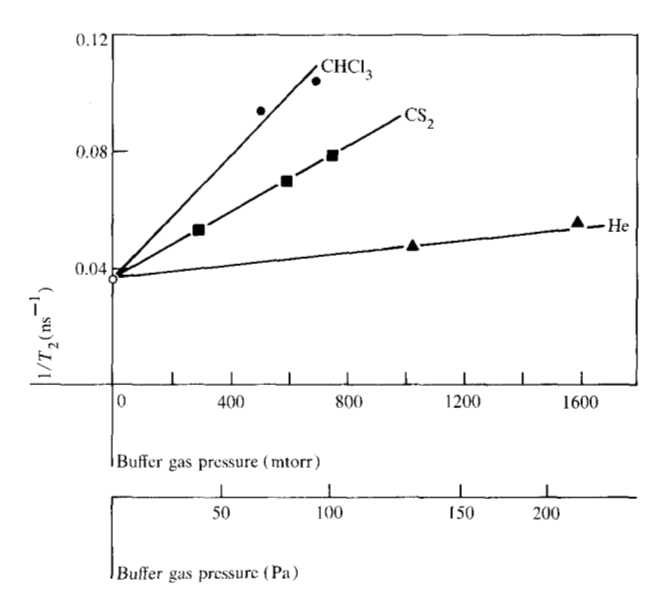


Figure 11 Plot of $1/T_2$ for 200 mtorr (27 Pa) of NH₃ with various buffer gases: $CHCl_3 \bullet$, $CS_2 \blacksquare$, and $He \blacktriangle$.

Table 1 NH, two-photon T_{a} , for various buffer gases.

	3 . 1	2		
Buffer gas	Two-photon transition $1/\pi T_2$ from this work (MHz/torr) [MHz/mPa]		Ground vibrational band linewidth from microwave measurement* (MHz/torr) [MHz/mPa]	
Не	3 ± 2	25 ± 15	2.6	20
Ar	3 ± 2	25 ± 15	3.4	26
N_2	11 ± 2	80 ± 15	7.6	57
CŠ ₂ CO ₂ SO ₂	18 ± 2	130 ± 15	13.0	98
CO,	21 ± 2	160 ± 15	13.6	102
SO,	25 ± 2	190 ± 15	24.0	180
CHCI ₃	33 ± 2	250 ± 15	40	300

^{*}From C. H. Townes and A. L. Schawlow, Microwave Spectroscopy, McGraw-Hill Book Co., Inc., New York, 1955.

We have also used this technique to study the effect of buffer gases on this two-photon transition in NH₃. The buffer gases included CHCl₃, SO₂, CO₂, CS₂, N₂, He, and Ar. Each buffer gas was mixed with 0.2 torr (\approx 27 Pa) of NH₃, and the two-photon dephasing relaxation time T_2 of this NH₃ transition was measured as a function of buffer gas pressure. Figure 11 shows a plot of $1/T_2$ versus the buffer gas pressure for three representative cases: CHCl₃ \bullet , CS₂ \blacksquare , and He \blacktriangle . The buffer gas collision-induced relaxation times for this two-photon transition can be obtained from such curves; the relaxation times are shown in Table 1.

We now discuss the physical origin of the dephasing process. Due to the well-known inversion doublets in

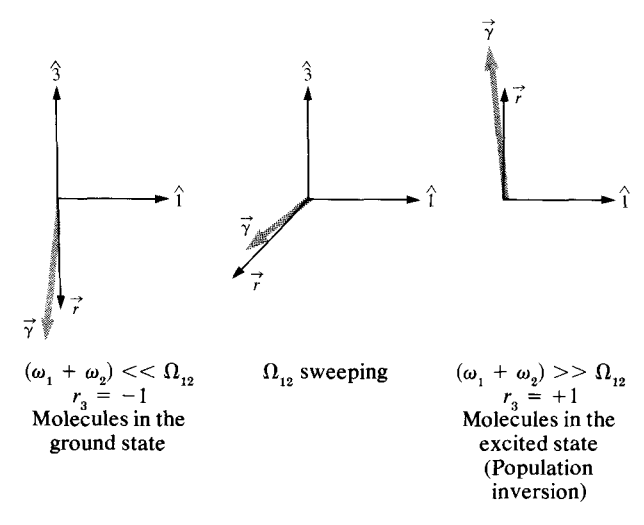


Figure 12 Schematic diagram of the adiabatic rapid passage method.

NH₃, the relaxations of the vibrational-rotational states are dominated by transitions between the doublets of the same J, K, and M values. Since the spacing of the doublets increases substantially for the excited ν_a bands (the spacing being about 0.8, 36, and 280 cm⁻¹ for the $\nu_a = 0.1$, and 2 bands, respectively), the relaxation times are also expected to increase. Thus, the two-photon relaxation times measured should be largely determined by the relaxation of the rotational states in the ground vibrational band. In Table 1 we show the NH₃ ground vibrational band relaxation times as determined by microwave spectroscopy together with the two-photon phase relaxation time. The two columns of relaxation times, while not equivalent, do follow the same ordering, indicating the dominant role of the $\nu_2 = 0$ band relaxation between the inversion doublets.

• Two-photon adiabatic inversion

One of the most interesting predictions of the two-photon vector model is the possibility of inverting the population of the two-photon transition by the technique of adiabatic rapid passage [27]. One-photon adiabatic inversion has previously been demonstrated in our laboratory [28]. In terms of the vector model for our simplified three-level system, the two conditions for adiabatic inversion are as follows: 1) Either the two-photon transition frequency or the sum of the two input laser frequencies must be swept through resonance in a time that is short compared to the population relaxation time T_1 ; and 2) the rate of the frequency sweep must be adiabatic, *i.e.*,

$$\frac{d\gamma_3}{dt} < (\kappa \varepsilon_1 \varepsilon_2)^2.$$

This adiabatic rapid passage process is represented in Fig. 12. Initially, with the system in the ground state and the excitation far off resonance, both $\vec{\gamma}$ and \vec{r} point along the $-\hat{3}$ axis. As the excitation sweeps through resonance, while maintaining the adiabatic condition, \vec{r} remains aligned with $\vec{\gamma}$. At the end of the passage process, with the excitation on the other side of resonance, $\vec{\gamma}$ now points along the $+\hat{3}$ axis. Since \hat{r} remains aligned with $\vec{\gamma}$, the population is totally inverted.

For this experiment, we again use the same two-photon transition in NH₃. In an early theoretical paper, Grischkowsky and Loy [27] suggested that by using the optical Stark effect to sweep through the two-photon transition while satisfying the adiabatic condition, one might obtain self-induced adiabatic rapid passage. In this experiment, instead of the self-induced approach, which depends critically on the laser pulse shape, the Stark switching technique was used. It was clearly shown in the two-photon free-precession experiments just described that the Stark switching technique, being electronically controlled, yielded stable signals that allowed one to obtain accurate relaxation information.

Conceptually, this experiment should be the same as the two-photon free-precession experiment except that the weak-field amplitude ε_2 should be increased to the same order as ε_1 . This should give a sufficiently large product of $\kappa \varepsilon_1 \varepsilon_2$ to satisfy the adiabatic condition. Such an ε_{0} can be easily obtained from another single-mode TEA laser identical to the one that provided ε_1 . Another attractive feature is that the optical Stark shifts due to ε_1 and ε_2 have opposite signs. When ε_1 and ε_2 are of the same order, the net shift is considerably reduced by cancellation. The main difficulty of this approach is the experimental detection of the two-photon transient signal, since both beams are equally strong and the expected signal-to-background ratio becomes extremely small. Theoretically, after the adiabatic passage, a third weak beam could be used to probe the two-photon population inversion. In practice, the experimental setup was much more complicated, and our initial attempts along this direction did not prove fruitful.

It became clear that the experiment should be attempted where the weak-beam/strong-beam configuration was maintained, but with several modifications. First, the output of the low-pressure CO_2 laser (weak beam) was increased to ≈ 3 kW/cm² by doubling the laser discharge length. Second, the 1- μ s single-mode TEA laser output (strong beam) was focused into the Stark cell at an intensity of 2.5 MW/cm². Third, in our previous Stark switched free-precession experiment the intensity of the strong beam was sufficiently low that the optical Stark

shift was much smaller than the zero-field frequency offset $\delta = 294$ MHz. Here, at the much higher strong-beam intensity, the optical Stark shift is about 2.5 times δ . In fact, had we continued to have the strong beam at P18, the optical Stark shift alone (without the external field) would have shifted the transition through resonance. To avoid this, the strong beam was changed to be at P34, while the weak beam was set at P18. Thus, the transition was shifted away from resonance by the strong beam. Because application of an external Stark pulse shifted the two-photon transition in the opposite direction, we could sweep through resonance in a controlled manner. Finally, to increase the size of the signal, the Stark cell was enlarged from 10 to 40 cm.

Typical results of the experiment are shown in Fig. 13 for two NH₃ pressures. The duration of the Stark pulse for both cases was about 210 ns with a field strength of 7650 V/cm. The shape of the Stark pulse was asymmetrical; it swept through resonance more slowly at the rising edge than at the trailing edge. Calculation showed that the excitation was adiabatic on the rising edge, but nonadiabatic on the trailing edge. In Fig. 13(a), the gas pressure was 100 mtorr (\approx 13 Pa), corresponding to a T_1 , shorter than the Stark pulse width. While the absorption signal at the trailing edge was smaller than that at the rising edge, there was no two-photon emission signal since the inverted population had substantially decayed during the Stark pulse. To observe emission one must probe the system at a time after inversion that is short compared to T_1 . This was achieved by performing the experiment with the same Stark pulse and laser intensities but at a lower NH_a pressure when the relaxation time T_1 is much longer. The result is shown in Fig. 13(b), where the NH₃ pressure was 9 mtorr (≈1 Pa). Here, in contrast to the trace in Fig. 13(a), when the system was probed at the trailing edge of the Stark pulse, a two-photon emission signal was clearly seen, demonstrating the population inversion of this twophoton transition in NH₃. Further, this coherent emission signal on the weak beam occurred only in the presence of the strong beam, showing that this is definitely stimulated two-photon emission and not one-photon emission to the intermediate state.

From experimental results such as those above, we can obtain for the first time the population relaxation time T_1 of a two-photon transition. In fact, for this transition in NH $_3$ we find that the population relaxation follows two distinct time constants. These correspond to the relaxation times of the $\nu_2=0$ and $\nu_2=2$ bands, which, as discussed earlier, are expected to be quite different. The measured time constants are 11.5 \pm 1 ns-torr (1.53 \pm 0.13 ns-kPa) and 35.5 ns-torr (4.72 ns-kPa) for the $\nu_2=0$ and $\nu_2=2$ bands, respectively.

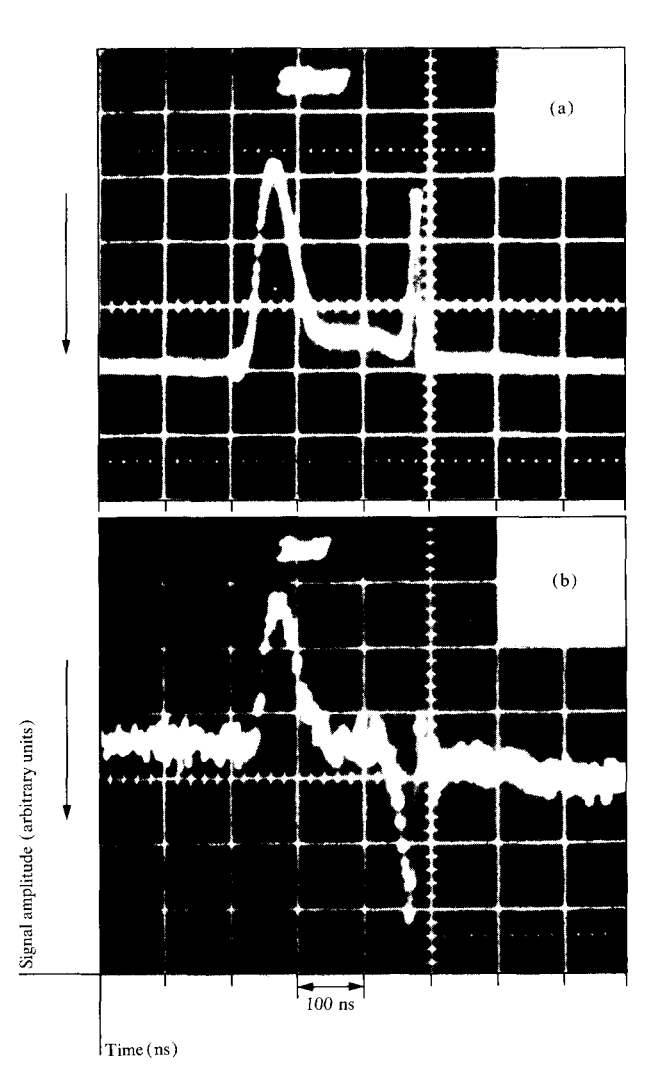


Figure 13 Two-photon adiabatic inversion in NH₃ as a function of pressure: (a) at 100 mtorr (\approx 13 Pa); (b) at 9 mtorr (\approx 1 Pa).

It has long been recognized that an inverted two-photon transition could lead to a two-photon laser [29], but experimentally this has yet to be realized. In fact, while the related stimulated anti-Stokes emission from an inverted Raman transition has been observed [30], stimulated emission from a two-photon transition in the optical regime [31] was observed for the first time in our experiment. While this system does not appear promising for the achievement of two-photon laser oscillation due to the small gain, this is a significant first step toward the continuing search for the two-photon laser.

D. Conclusion

We have demonstrated that two-photon analogues of the familiar one-photon transients can be easily observed. With the aid of the two-photon vector model of Grisch-

kowsky, Loy, and Liao, these apparently complicated effects can be conveniently visualized and understood. The predictions of this vector model were quantitatively confirmed by our experimental results.

In addition to demonstrating the experimental existence of these novel two-photon transients, we have also exploited them as techniques to measure the relaxations T_1 and T_2 of two-photon transitions, which are not accessible by one-photon excitations.

We should point out that all of our data were obtained from single-shot experiments, with the data taken from oscilloscope traces. Even with this somewhat unsophisticated method, precise measurements of relaxation times were obtained. It is obvious that with some equipment improvements, such as higher-repetition-rate lasers and more sophisticated detection methods, we can expect significant improvements in our experiments. Toward this end we have constructed a CO₂ TEA laser capable of repetition rates of 10-20 Hz at up to 1 J per pulse. Instead of taking pictures of scope traces, we plan to use a transient digitizer such as the Tektronix 7912 AD. This transient digitizer will be interfaced with a computer so that digital signal averaging can be used. It is hoped that the potentials of these two-photon coherent techniques will be more fully realized by such improvements.

At present, imperfections of the laser sources and the special skills needed to operate these sources are still barriers to wider application of these coherent optical effects. However, one should note the tremendous improvements in laser technology since the invention of lasers nearly twenty years ago. It is perhaps not unrealistic to expect that future laser sources could be just as reliable, tunable, and easy to use as rf and microwave sources. Thus, it appears likely that these one- and two-photon coherent transient techniques can become important analytical tools.

Acknowledgment

This work was partially supported by the Office of Naval Research, Washington, DC, under Contract No. N00014-76-C-0907.

References and notes

- 1. See, e.g., A. Abragam, The Principles of Nuclear Magnetism, Oxford University Press, Oxford, England, 1961.
- See, e.g., L. Allen and J. H. Eberly, Optical Resonance and Two-Level Atoms, John Wiley & Sons, Inc., New York, 1975.

- 3. R. G. Brewer and R. L. Shoemaker, *Phys. Rev. Lett.* **27**, 63 (1971); R. G. Brewer and A. Z. Genack, *Phys. Rev. Lett.* **36**, 959 (1976); R. G. Brewer, *Phys. Today* **30**, 50 (1977); A. Z. Genack and R. G. Brewer, *Phys. Rev. A* **17**, 1463 (1978); and R. G. DeVoe and R. G. Brewer, *IBM J. Res. Develop.* **23**, 529 (1979), this issue).
- R. P. Feynman, F. L. Vernon, Jr., and R. W. Hellwarth, J. Appl. Phys. 28, 49 (1957).
- 5. S. R. Hartmann, IEEE J. Quantum Electron. QE-4, 802 (1968)
- E. M. Belenov and I. A. Poluektov, Zh. Eksp. Teor. Fiz. 56, 1407 (1969) [Sov. Phys. JETP 29, 754 (1969)].
- 7. M. Takatsuji, Phys. Rev. A 11, 619 (1975).
- 8. R. G. Brewer and E. L. Hahn, Phys. Rev. A 11, 1614 (1975).
- D. Grischkowsky, M. M. T. Loy, and P. F. Liao, *Phys. Rev.* A 12, 2514 (1975).
- R. L. Shoemaker and R. G. Brewer, *Phys. Rev. Lett.* 28, 1430 (1972).
- M. Matsuoka, H. Nakatsuka, and J. Okada, *Phys. Rev. A* 12, 1062 (1975).
- 12. M. M. T. Loy, Phys. Rev. Lett. 36, 1454 (1976).
- P. Hu, S. Geschwind, and T. M. Jedju, *Phys. Rev. Lett.* 37, 1357, 1773(E) (1976).
- P. F. Liao, J. E. Bjorkholm, and J. P. Gordon, *Phys. Rev. Lett.* 39, 15 (1977).
- 15. M. M. T. Loy, Phys. Rev. Lett. 39, 187 (1977).
- B. Cagnac, M. Bassini, F. Biraben, and G. Grynberg, in Laser Spectroscopy III, J. L. Hall and J. L. Carlsten, Eds., Springer-Verlag, New York, 1977.
- P. F. Liao, N. P. Economou, and R. R. Freeman, *Phys. Rev. Lett.* 39, 1473 (1977).
- T. Mossberg, A. Flusberg, R. Kachru, and S. R. Hartmann, *Phys. Rev. Lett.* 39, 1523 (1977).
- 19. A. Flusberg, T. Mossberg, R. Kachru, and S. R. Hartmann, *Phys. Rev. Lett.* 41, 305 (1978).
- 20. M. M. T. Loy, Phys. Rev. Lett. 41, 473 (1978).
- H. Hatanaka and T. Hashi, J. Phys. Soc. Japan 39, 1139 (1975); H. Hatanaka, T. Ozawa, and T. Hashi, J. Phys. Soc. Japan 42, 2069 (1977).
- 22. D. G. Gold and E. L. Hahn, Phys. Rev. A 16, 324 (1977).
- 23. W. Heitler, The Quantum Theory of Radiation, Oxford University Press, London, 1954.
- 24. H. Friedmann and A. D. Wilson-Gordon, Opt. Commun. 24, 5 (1978).
- 25. A. Schenzle and R. G. Brewer, Phys. Reports 43, 455 (1978).
- M. M. T. Loy and P. A. Roland, Rev. Sci. Instrum. 48, 554 (1977).
- 27. D. Grischkowsky and M. M. T. Loy, *Phys. Rev. A* 12, 1117 (1975).
- 28. M. M. T. Loy, Phys. Rev. Lett. 32, 814 (1974).
- P. P. Sorokin and N. Braslau, IBM J. Res. Develop. 8, 177 (1964). See also R. L. Carman, Phys. Rev. A 12, 1048 (1975) and references therein.
- P. P. Sorokin, N. S. Shiren, J. R. Lankard, E. C. Hammond, and T. G. Kazyaka, Appl. Phys. Lett. 10, 44 (1967); R. L. Carman and W. H. Lowdermilk, Phys. Rev. Lett. 33, 190 (1974)
- 31. Stimulated phonon-photon two-quantum emission has been observed by N. S. Shiren, *Appl. Phys. Lett.* 7, 142 (1965).

Received January 29, 1979; revised March 15, 1979

The author is located at the IBM Thomas J. Watson Research Center, Yorktown Heights, New York 10598.